Journal of Catalysis **200,** 10–20 (2001)
doi:10.1006/jcat.2001.3191, available online at http://www.idealibrary.com on IDEAL®

Effect of the Type of Activated Carbons on the Photocatalytic Degradation of Aqueous Organic Pollutants by UV-Irradiated Titania

J. Matos,*,† J. Laine,† and J.-M. Herrmann*,[1]

*Laboratoire de Photocatalyse, Catalyse et Environnement, IFoS (UMR au CNRS), Ecole Centrale de Lyon, BP 163, 69131 Ecully Cédex, France; and †Laboratorio de Fisicoquímica de Superficies, Centro de Química, Instituto Venezolano de Investigaciones Científicas, Apartado 21827, Caracas 1020-A, Venezuela

Received May 24, 2000; revised October 30, 2000; accepted January 31, 2001; published online April 18, 2001

The photocatalytic degradation of three model pollutants (phenol, 4-chlorophenol, and herbicide 2,4-D (2,4-dichlorophenoxyacetic acid) was performed at room temperature in aqueous suspended mixtures of TiO_2 and of two different activated carbons (AC) of commercial origin. The kinetics of disappearance of the pollutants followed an apparent first-order rate, whose constant was selected as the best parameter (independent of pollutant concentrations) to determine the influence of each AC on the photoactivity of titania. Remarkable different effects were observed in the kinetics of disappearance of the pollutants as well as in the kinetics of appearance and disappearance of the intermediate products detected. Each pollutant was more rapidly photodegraded in the mixed system which contained H-type activated carbon. In the case of phenol, a maximum synergy factor R equal to 2.5 was detected when the mass ratio ($TiO_2/AC_{H\text{-type}}$) corresponded to (50/10). An identical synergy factor (2.4) was found for 4-chlorophenol degradation, whereas a smaller one ($R = 1.3$) was found for 2,4-D because of its poor solubility. On the contrary, the L-type activated carbon inhibited titania's photoactivity with $R < 1$. In addition, significant differences in intermediate product distributions were observed as a function of the type of AC. The synergy or inhibition effects and the formation of the different intermediate products detected have been correlated to the origins and the properties of the two AC employed. When performing the "helio-photocatalytic" degradation of 4-chlorophenol with an extrapolation volume factor of 12,500 in a large-scale solar pilot plant, an identical synergy factor of 2.4 was found, thus confirming the transpositivity of laboratory experiments to large solar setups. The synergy effect was not destroyed when reusing the double-phase photocatalyst. This photocatalytic system, associating titania with H-type activated carbon, may appear as a new performing one, more efficient with a shorter time necessary for decontaminating diluted used waters. It could be of interest in producing detoxified and/or drinking water in dry sunny areas.

Key Words: **photocatalysis; helio-photocatalysis; titania; organic pollutants degradation; activated carbon; phenol; 4-chlorophenol; 2,4-D; associative effect.**

1. INTRODUCTION

One of the most important challenges for science is to develop efficient methods to control environmental pollution. In the case of polluted waters, heterogeneous photocatalysis recently emerged as an efficient purifying method (1–7). Up to now, in more than 1700 references that have been recently collected on this discipline (5), titania under the shape of anatase has always been found as the best photocatalyst. Several attempts have been made to increase its photoefficiency either by noble metal deposition (8) or by ion doping (8, 9), but such modifications did not enhance the photocatalytic activity of titania and were rather detrimental. A third way to possibly increase the photocatalytic efficiency of titania consists of adding a coadsorbent such as silica, alumina, zeolites, or clays (10–12), but no improvement of photoefficiency was observed (11, 12). Activated carbon is another type of coadsorbent that has been used either in gas phase (13–15) or in aqueous phase (11, 12, 15–17) in the photodegradation of organic pollutants. We have already observed a synergy effect when using powdered titania and a powdered activated carbon in the photocatalytic degradation of phenol (18). This synergistic effect was ascribed to the creation of a common contact interface between both solid phases and to a transfer of phenol adsorbed on activated carbon (AC) to titania where it was immediately photocatalytically degraded. The aim of the present study was to extend the study of the synergy effect to two different activated carbons (one of the H-type and the other of the L-type, H and L for high-temperature ("physical") and low-temperature ("chemical") method of activation, respectively) and to three model pollutants (Ph, phenol; 4-cp, 4-chlorophenol; and herbicide 2,4-D, 2,4-dichlorophenoxyacetic acid).

2. EXPERIMENTAL

2.1. Materials

The three model pollutants mentioned above and the main intermediate products detected (hydroquinone (HQ),

[1] To whom correspondences should be addressed. E-mail: jean-marie.herrmann@ec-lyon.fr.

0021-9517/01 $35.00

TABLE 1

Some Characteristics of Commercial Merck (AC_M) and Purocarbon (AC_{PC}) Activated Carbons

AC	Mean pore width[a] (nm)	$Total_{BET}$ surface area (m^2/g)	Micropore surface area[b] (m^2/g)	Ash (%)
AC_M	0.8	775	649	<1
AC_{PC}	1.9	1240	775	2.5[c]

[a] Measured by the Horrwarth–Kawazoe method.

[b] Surface area related to pores with diameter <2 nm, measured by the *t*-plot method.

[c] Principally phosphorus-containing oxides remaining from the "chemical" activation.

benzoquinone (BQ), cathecol (CT), resorcinol (RS), 4-chlorocathecol (4-CCT), 4-chlororesorcinol (4-CRS), 2-chlorohydroquinone (2-CHQ), and 2,4-DCP) were purchased from Aldrich with the highest purity grade and used as received. The photocatalyst was TiO_2 Degussa P-25, mainly anatase (ca. 70%) under the shape of nonporous polyhedral particles of ca. 30-nm mean size with a surface area of 50 m^2/g. Two different commercial activated carbons were studied: a high-purity activated carbon purchased from Merck (AC_M), already used by some of us for supporting hydrodesulfuration (19) and hydrogenation (20) catalysts, and a second one with the commercial name of Purocarbon (AC_{PC}). Some properties of those activated carbons are shown in Table 1.

2.2. Photoreactor and Light Source

The batch photoreactor was a cylindrical flask made of Pyrex of ca. 100 mL with a bottom optical window of ca. 4 cm in diameter and was open to air. It has been previously shown that stirring the suspension in air provided enough oxygen for the oxidative photodegradation. Irradiation was provided by a high-pressure mercury lamp (Phillips HPK, 125 W) and was filtered by a circulating-water cell (thickness, 2.2 cm) equipped with a 340-nm cutoff filter (Corning 0.52).

2.3. Analysis

Millipore disks (0.45 μm) were used to remove particulate matter before HPLC analysis. The HPLC system comprised a LDC/Milton Roy Constametric 3200 isocratic pump and a Waters 486 tunable absorbance detector (Millipore) adjusted at 270, 280, and 283 nm for the detection of Ph, 4-CP, and 2,4-D, respectively, and of the main intermediate products. A reversephase column (length, 250 mm; i.d., 4.6 mm; particle diameter, 5 mm) ODS2-Spherisorb (Chrompack) was used. The mobile phases were composed of acetonitrile/water (v/v ratio equal to 10/90), methanol/water (40/60), and methanol/water (55/45) for Ph, 4-CP, and 2,4-D analyses, respectively.

3. RESULTS

3.1. Photodegradation of Phenol

3.1.1. Adsorption in the dark. Preliminary studies of phenol adsorption at 20°C were performed on neat titania (50 mg), AC_M (10 mg), AC_{PC} (10 mg), and the suspended mixtures TiO_2–AC_M and TiO_2–AC_{PC} with the same respective masses. The kinetics of adsorption in the dark were followed for 1.5 h under stirring for different initial concentrations between 10^{-4} and 10^{-2} mol/L. The kinetics of phenol's adsorption in the dark for those systems are given in Fig. 1 for an initial concentration $C_0 = 10^{-3}$ mol/L (94 ppm). In all cases, most of adsorption occurred within 15 min. The adsorption isotherms $n_{ads} = f(C_{eq})$ were determined by assuming the conventional Langmuir isotherm model with a surface coverage θ varying as

$$\theta = (n_{ads}/n_T) = \{K_{ads} \cdot C/(1 + K_{ads} \cdot C)\}. \qquad [1]$$

The total number of adsorption sites n_T and the adsorption constants K_{ads} were obtained from the linear transform $(1/n_{ads}) = f(1/C_{eq})$, obtaining correlation coefficients close to 0.99. The corresponding values are given in Table 2.

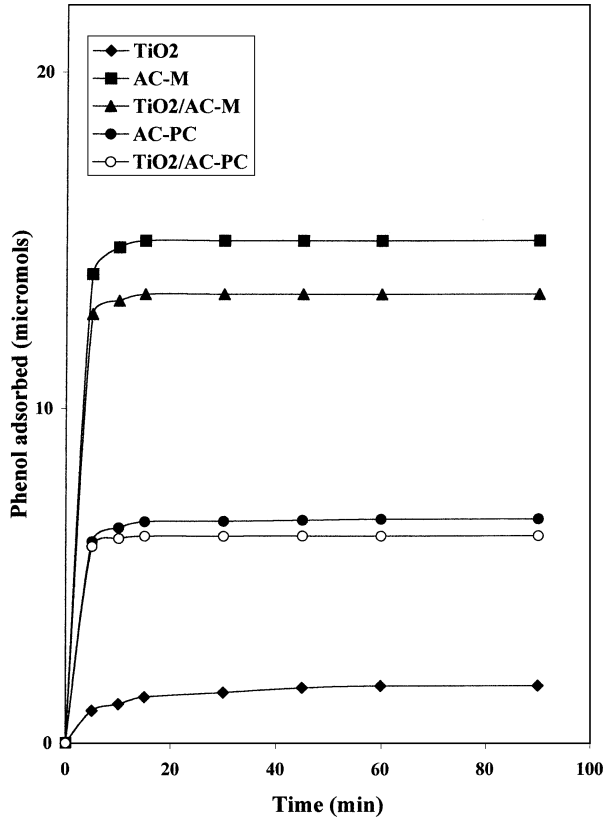

FIG. 1. Kinetics of phenol adsorption in the dark for $C_0 = 10^{-3}$ mol/L. TiO_2 (50 mg), AC_M (10 mg), AC_{PC} (10 mg), TiO_2–AC_M (50/10), and TiO_2–AC_{PC} (50/10).

TABLE 2

Adsorption Constant (K_{ads}) and Total Number of Adsorption Sites (n_T) for Phenol Adsorbed in the Dark, assuming a Langmuir Isotherm

Solids	K_{ads} (L/mol)	n_T (mol)
TiO_2	3.14×10^3	3.49×10^{-6}
AC_M	1.42×10^5	1.94×10^{-5}
TiO_2–AC_M	1.66×10^5	1.77×10^{-5}
AC_{PC}	2.32×10^3	9.69×10^{-6}
TiO_2–AC_{PC}	1.79×10^3	1.06×10^{-5}

Figure 1 shows that the numbers of moles of phenol adsorbed on TiO_2–AC_M and on TiO_2–AC_{PC} are smaller than these adsorbed on both ACs alone. Remarkable differences were detected when phenol adsorption parameters (K_{ads} and n_T) obtained on the mixed systems were compared with those of both ACs considered separately. When comparing TiO_2–AC_M with AC_M, the total number of adsorption sites decreased by 9% and the adsorption constant increased by ca. 17%. By contrast, the comparison of TiO_2–AC_{PC} with AC_{PC} indicated an increase of ca. 9% in the total number of adsorption sites and a decrease of ca. 23% in the adsorption constant. This contradiction can be ascribed to the different properties of each AC. It is in agreement with the fact that, although the surface area of AC_{PC} is higher than the surface area of AC_M (1240 vs 775 m^2/g), the total number of adsorption sites obtained on pure AC_M is twice higher than that on AC_{PC} and, in addition, its adsorption constant is ca. 60 times higher (Table 2).

3.1.2. Kinetics of the photocatalytic disappearance of phenol. It can be observed from Fig. 2 that both direct photolysis (i.e., without solids) and phenol decomposition in the presence of UV-irradiated AC_M or AC_{PC} without titania can be neglected. Pure titania gives a complete disappearance of phenol in about 6 h of UV irradiation. The behaviors of the irradiated mechanical mixtures TiO_2–AC_M and TiO_2–AC_{PC} were different. TiO_2–AC_M totally eliminated phenol from the solution within 3 h, whereas TiO_2–AC_{PC} required 9 h of continuous UV irradiation for a total disappearance of phenol from the solution.

The apparent rate constant has been chosen as the basic kinetic parameter to compare the different systems, *since it is independent of the concentration* and, therefore, enables one to determine the photocatalytic activity independently of the previous adsorption period in the dark. The kinetic curves of Fig. 2 are of apparent first order as confirmed by the correlation coefficients (close to 0.99), obtained from the linear transforms $\ln(n_0/n) = f(t)$ of Fig. 3, giving apparent rate constants equal to

$$TiO_2\ k_{app} = 0.56 \times 10^{-2}\ min^{-1}$$
$$TiO_2\text{–}AC_M\ k_{app} = 1.39 \times 10^{-2}\ min^{-1}$$
$$TiO_2\text{–}AC_{PC}\ k_{app} = 0.46 \times 10^{-2}\ min^{-1}.$$

The photocatalytic activity of TiO_2–AC_M was higher than that of neat titania, the addition of 10 mg AC_M to 50 mg TiO_2 created a positive associative (synergy?) effect with an increase of the rate constant by a factor of ca. 2.5. By contrast, the addition of the same weight of AC_{PC} was found detrimental.

The influence of the mass of titania upon the rate of phenol disappearance has been followed in the absence and in the presence of 10 mg AC_M or AC_{PC}. All the results are listed in Table 3, which indicates that, in all cases, the mixed system TiO_2–AC_M developed a beneficial effect on the kinetics of phenol photodegradation with an optimum for a mass ratio (TiO_2/AC_M) equal to (50/10). In contrast, for TiO_2–AC_{PC}, AC_{PC} inhibited titania's photoactivity with a factor practically constant, equal to 0.8, and independent of the mass of titania employed. It must to be noted that the highest apparent rate constants for TiO_2, TiO_2–AC_M, and TiO_2–AC_{PC} as a function of the mass of titania have always been found for 50 mg of the semiconductor. This optimum content of 50 mg TiO_2 for a constant mass of 10 mg AC corresponds to the situation where all the particles of TiO_2 are illuminated, depending on the geometry of the

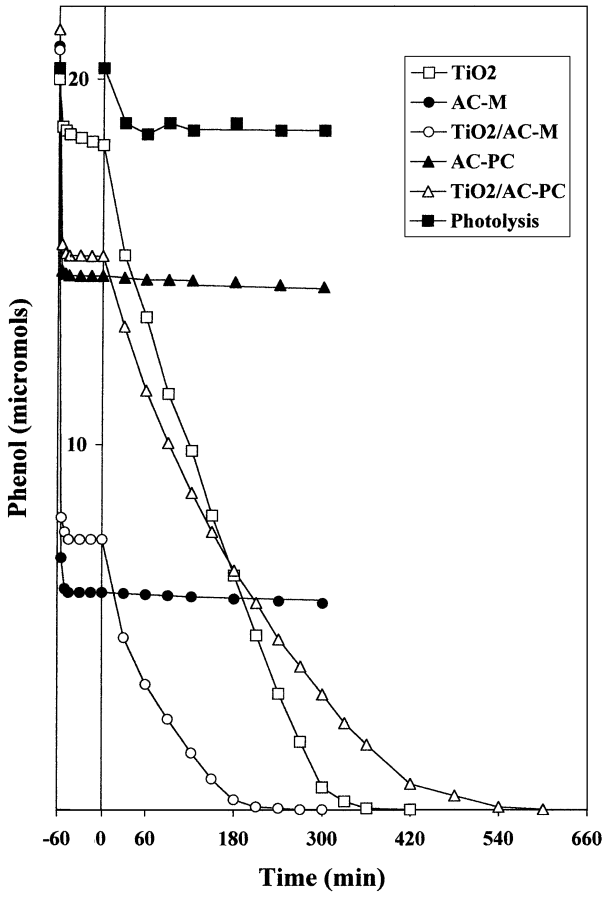

FIG. 2. Kinetics of phenol disappearance in the presence of the various illuminated solids in Fig. 1. The vertical line at time $t = 0$ separates the dark period from the UV-irradiated one.

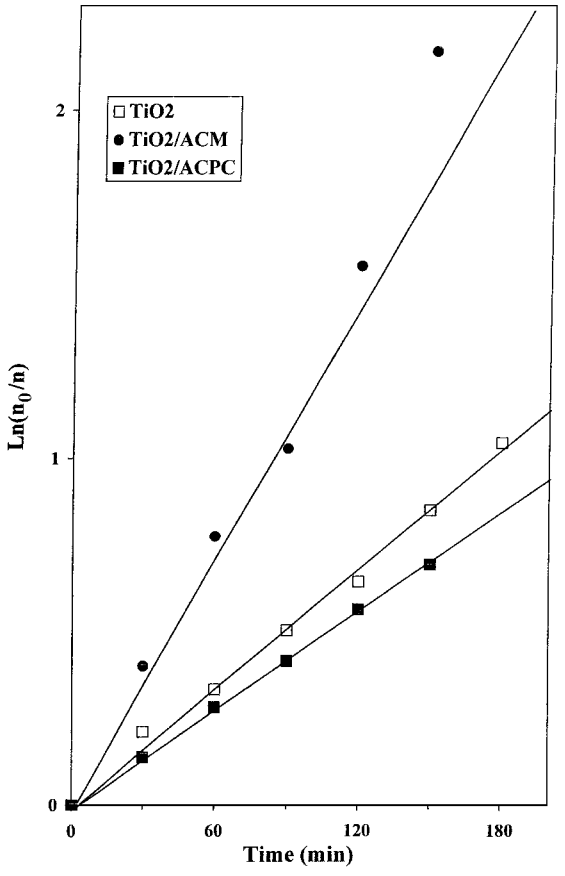

FIG. 3. Apparent first-order linear transform $\ln(n_0/n) = f(t)$ of the kinetic curves of phenol disappearance for TiO_2, TiO_2–AC_M, and TiO_2–AC_{PC} from Fig. 2.

photoreactor and on the light flux (6, 7). The decrease in activity observed beyond 50 mg TiO_2 is thought to be related to an increased scattering of photons out of the reactor due to an increased catalyst concentration near the reaction wall as already discussed (21).

3.1.3. Kinetics of appearance and disappearance of phenol's degradation intermediate products. All the results are presented in Fig. 4. As expected, HQ was the main intermediate product observed in all the systems studied. HQ exhibits a maximum substantially lower on TiO_2–AC_M than on neat titania and at a shorter reaction time. This is indicative of higher rates of HQ appearance and disappearance in line with what has been observed for the kinetics of phenol disappearance. Therefore, the beneficial effect due to the addition of 10 mg AC_M to 50 mg TiO_2 is confirmed. On the contrary, the maximum amount of HQ detected with illuminated TiO_2–AC_{PC} was higher than that observed on neat titania and detected at a greater reaction time. Similar features were also observed for BQ, the intermediate product resulting from the oxidation of HQ. In addition, significant changes in the intermediate product distributions were detected as a function of the type of AC added to TiO_2. For example, RS was also quantitatively detected on TiO_2 and

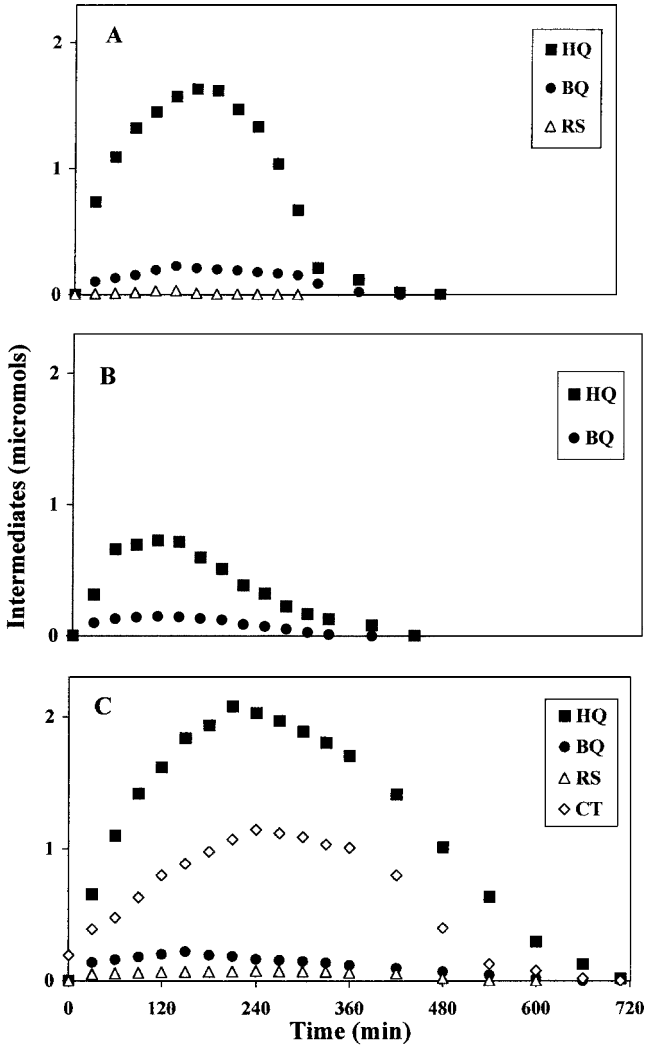

FIG. 4. Kinetics of appearance and disappearance of the main intermediate products detected during the photodegradation of phenol. (A) TiO_2 (50 mg), (B) TiO_2–AC_M (50/10), (C) TiO_2–AC_{PC} (50/10).

TABLE 3

Influence of the Mass of Titania upon the Apparent First-Order Rate Constants in Phenol Disappearance

Mass (mg)	$k_{app}(TiO_2)$ (min^{-1})	$k_{app}(TiO_2$–$AC_M)$ (min^{-1})	$k_{app}(TiO_2$–$AC_{PC})$ (min^{-1})	$R > 1$	$R < 1$
75	0.37×10^{-2}	0.49×10^{-2}	0.29×10^{-2}	1.32	0.78
50	0.56×10^{-2}	1.39×10^{-2}	0.46×10^{-2}	2.48	0.82
30	0.51×10^{-2}	1.07×10^{-2}	0.41×10^{-2}	2.10	0.80
20	0.47×10^{-2}	0.91×10^{-2}	—	1.94	—
10	0.40×10^{-2}	0.70×10^{-2}	—	1.75	—
5	0.33×10^{-2}	0.43×10^{-2}	—	1.30	—
0	0	0	0	0	0

Note. $R = \{k_{app}(TiO_2$–$AC)/k_{app}(TiO_2)\}$ = synergy ($R > 1$) or inhibition ($R < 1$) factor.

TiO_2–AC_{PC} but in much smaller quantities than HQ or BQ. Moreover, the intermediate product cathecol (CT) was only detected on TiO_2–AC_{PC}.

3.2. Photodegradations of 4-Chlorophenol and of 2,4-Dichlorophenoxyacetic Acid

The kinetics of adsorption in the dark of 4-CP and 2,4-D were followed for 1.5 h while stirring TiO_2, AC_M, AC_{PC}, TiO_2–AC_M, and TiO_2–AC_{PC} suspensions for an initial concentration equal to 10^{-3} mol/L for 4-CP and to 5×10^{-4} mol/L only for 2,4-D, because of the poor solubility of 2,4-D in water. The low solubility of 2,4-D favored its quasi-complete adsorption on AC. This is why the mass of AC had to be decreased twice to 5 mg to limit adsorption for a satisfactory detection in the solution leading to a correct kinetic study. In that case, the mass ratio of TiO_2/AC_M was chosen equal to 50/5.

Both pollutants followed the same decreasing order as phenol for adsorption in the dark:

$$AC_M > TiO_2\text{–}AC_M > AC_{PC} > TiO_2\text{–}AC_{PC} > TiO_2.$$

4-CP and 2,4-D were completely eliminated from the solution during UV-irradiation periods shorter for TiO_2–AC_M than for neat titania and for TiO_2–AC_{PC} (Figs. 5 and 6). The photocatalytic activity of TiO_2–AC_M was significantly higher than that obtained with neat titania for all the molecules studied (Table 4). On the contrary, the photocatalytic activity of TiO_2–AC_{PC} was smaller than that of TiO_2 alone, especially for 2,4-D degradation. In other words, the photocatalytic behaviors of the mixed systems are completely opposite according to the physical nature of ACs used.

The kinetics of appearance and disappearance of the main intermediate products detected during the photocatalytic degradation of 4-CP and of 2,4-D were also followed. 4-CP mainly gave HQ and 4-CRS and, additionally, traces of 4-CCT in the case of TiO_2–AC_{PC}. The aromatic intermediates produced during 2,4-D decomposition, principally 2,4-DCP and 2-CHQ, are presented in Table 5. The distributions of the intermediate products (HQ, BQ, 4-CRS 4-CCT, 2,4-DCP) varied with the type of AC employed conjointly with titania. These differences are explained under Discussion.

3.3. Extension to "Helio-photocatalysis"

The above experiments relative to 4-CP photocatalytic degradation have been transposed to the solar Compound Parabolic Collector (CPC) pilot photoreactor at the Solar Platform in Almeria (PSA) Spain, using a total volume of 247 L, which represents a volume extrapolation factor of 12,500. The titania concentration was chosen equal to 0.2 g/L, corresponding to the minimum optimal concentration of Degussa P-25. The mass ration AC_M/TiO_2 was kept

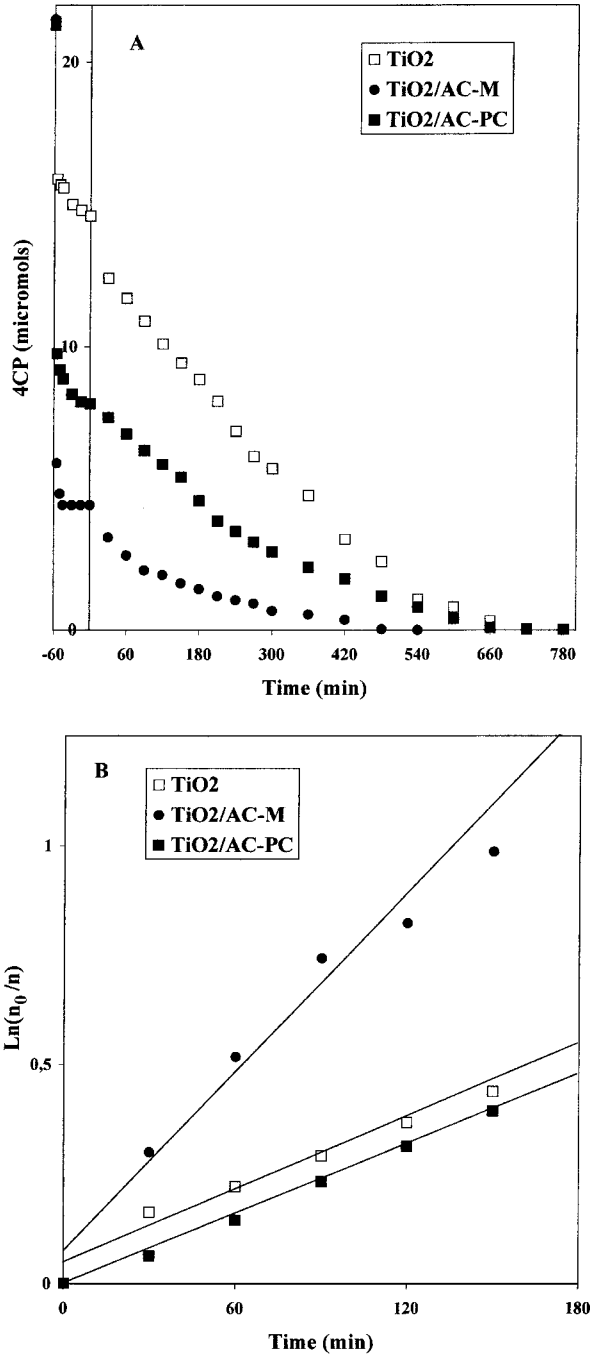

FIG. 5. (A) Kinetics of 4-chlorophenol disappearance in the presence of TiO_2, TiO_2–AC_M, and TiO_2–AC_{PC}. (B) Apparent first-order linear transforms $\ln(n_0/n) = f(t)$ of the kinetic curves from part A.

equal to 1/5, and the initial concentration of 4-CP was chosen equal to 20 ppm (1.55×10^{-4} mol/L).

It was first confirmed that the AC–TiO_2 mixture adsorbed much more 4-CP in the dark than titania alone. The disappearance of 4-CP was followed as a function of the residence time t_R corresponding to the time really spent in the CPC collector ($t_R = t\ (V_{collector}/V_{Total})$) and as a function of the

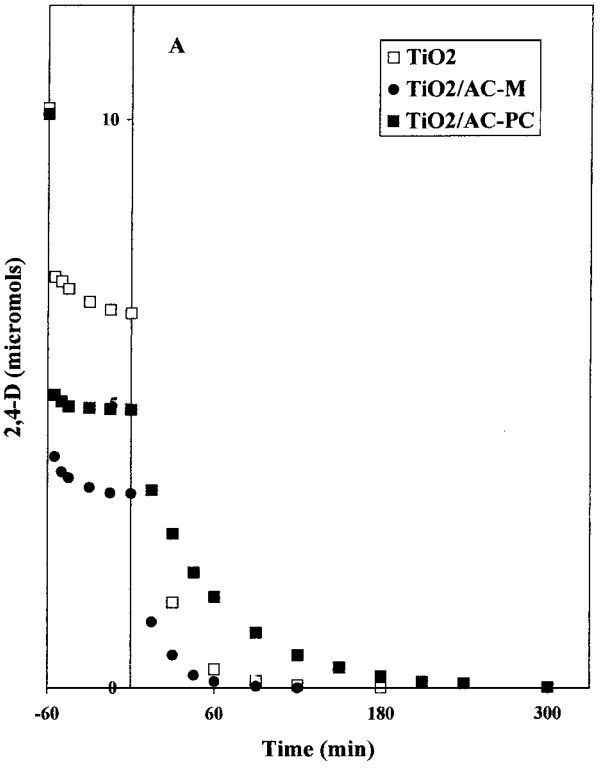

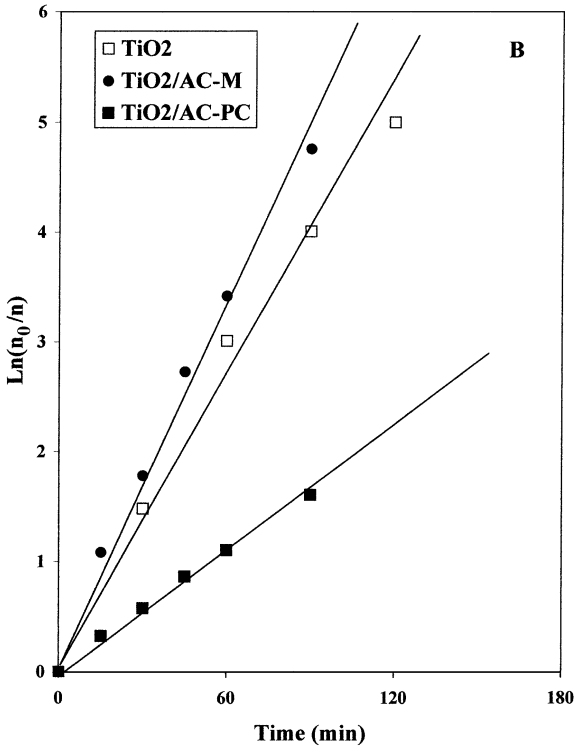

FIG. 6. (A) Kinetics of 2,4-D disappearance in the presence of TiO_2, TiO_2–AC_M, and TiO_2–AC_{PC}. (B) Apparent first-order linear transforms $\ln(n_0/n) = f(t)$ of the kinetic curves from part A.

TABLE 4

Apparent First-Order Rate Constants of the Photodegradation of Ph, 4-CP, and 2,4-D on UV-Irradiated TiO_2, TiO_2–AC, and TiO_2–AC_{PC}

Pollutant	TiO_2	TiO_2–AC_M	TiO_2–AC_{PC}
Ph	0.56×10^{-2}	1.39×10^{-2}	0.46×10^{-2}
4-CP	0.27×10^{-2}	0.64×10^{-2}	0.27×10^{-2}
2,4-D	4.17×10^{-2}	5.24×10^{-2}	1.77×10^{-2}

solar exposure in order to correct any possible variations of the solar radiant flux induced by the earth rotation during the experiment and by the possible occurrence of clouds in the sky. As in laboratory experiments, a 4-CP-free water was obtained in a shorter time when adding AC_M. Factor R ($R = k_{app}(TiO_2–AC_M)/k_{app}(TiO_2)$) was found identical to that found in laboratory experiments: $R = 2.4$. This positive effect is responsible for a lower content of intermediates in the solution and for a shorter solar exposure necessary to reach a total TOC disappearance. The reproducibility of factor R in a quite different experimental device clearly demonstrates that R is not relevant of any artifact.

4. DISCUSSION

4.1. TiO_2–AC Interface

For all three pollutants, the slurry mixture does not provide an additive effect in adsorption capacities of both solids. the slightly smaller adsorption in the case of TiO_2–AC is indicative of a competition between the pollutants and titania for approaching the AC's surface, which could

TABLE 5

Maximum Quantities of the Intermediate Products Detected

		Maximum quantity (μmol)		
Pollutant	Intermediate	TiO_2	TiO_2–AC_M	TiO_2–AC_{CP}
Phenol	HQ	1.63	0.73	2.08
	BQ	0.23	0.15	0.22
	RS	0.03	0	0.07
	CT	0	0	1.15
	Total	1.89	0.88	3.52
4CP	HQ	0.30	0.22	1.01
	BQ	0	0	0.08
	4CRS	0.07	0	0.03
	4CCT	0	0	0.34
	Total	0.37	0.22	1.46
2,4-D	2CHQ	0.13	0.07	0.15
	4CCT	0	0	0.02
	2,4-DCP	0.84	0.07	0.05
	Total	0.97	0.14	0.22

be interpreted by the creation of an interface between TiO_2 and AC at which pollutant molecules cannot adsorb. The contact area ΔS of this common interface can be estimated from the adsorption data according to the formula

$$\Delta S = \Delta n/[d_{(TiO_2)} + d_{(AC)}], \quad [2]$$

where $d_{(TiO2)}$ and $d_{(AC)}$ represent the respective surface densities in adsorbed pollutant (in mol/m^2) at the same final equilibrium concentration ($C_{eq} = 3.31 \times 10^{-4}$ mol/L for phenol) and where Δn is the difference between the sum of the adsorption capacities of the two solids considered separately and the adsorption capacity of their mixture. ΔS depends on the relative amounts of titania and AC (Table 6). Similar ΔS values were obtained from adsorption of the other two pollutants.

4.2. *Association and Inhibition Effects for TiO_2–AC_M and TiO_2–AC_{PC}, Respectively*

4.2.1. Case of TiO_2–AC_M. The association between TiO_2 and AC_M during the photocatalytic degradation of the three pollutants clearly appears in all the kinetic curves presented above (Figs. 2–4). It has been reasonably quantified by calculating the ratio of the apparent first-order rate constants of pollutant disappearance:

$$[k_{app}(TiO_2{-}AC)/k_{app}(TiO_2)] = 2.5. \quad [3]$$

Even if active carbon perturbs the transmission of UV light to the surface of titania, it largely compensates this inhibition by a strong beneficial effect in phenol adsorption followed by a transfer of phenol to titania. The driving force for this transfer is probably the difference in phenol concentration between AC and TiO_2 that causes surface diffusion of phenol to titania. The surface diffusion and the intimate contact between titania and AC have been proven by the pollutant transfer from AC to TiO_2 at the end of the pollutant disappearance in water. This was done by measuring the decreasing quantities of pollutants remaining on AC (after selective extraction in acetonitrile) as a function of supplementary irradiation time as developed in Ref. 18 (Section 4.3) and illustrated by Fig. 8 in the same Ref. 18. As a consequence, we have to deal with an association of both phases. The intimate contact between titania and AC is also corroborated by the fact that factor R is almost independent of the pollutant (i.e., phenol vs 4-CP) and quite independent of the photoreactor design (20 mL vs 247 L) and of the light source (artificial vs solar UV light). The interfacial contact areas ΔS created between TiO_2 and AC_M were varied as a function of TiO_2 masses employed in the interval between 5 and 50 mg, since this interval corresponds to the region of increasing photoactivity (see Table 3). Table 6 shows the synergy factors R (listed in Table 3) and the estimated interfacial common areas.

TABLE 6

Influence of Interfacial Areas (ΔS) on Factor R in Phenol Photodegradation on UV-Irradiated TiO_2–AC_M

Ratio mass (TiO_2/AC_M)	ΔS (m^2)	R
5/10	0.34	1.30
10/10	0.53	1.75
20/10	0.77	1.94
30/10	0.97	2.10
50/10	1.26	2.48
75/10	1.72	1.32

Note. $R = \{k_{app}(TiO_2{-}AC_M)/\ k_{app}(TiO_2)\}$.

The influence of the interfacial area upon factor R is presented in Fig. 7. The point relative to the mixture with a mass ratio (TiO_2/AC_M) equal to (75/10) was omitted since titania is in excess and has a detrimental effect as described in Section 3.1.2. In Fig. 7, both parameters follow a linear relationship with a correlation coefficient close to 0.99, given by the equation

$$R = 0.99 + 1.20\Delta S. \quad [4]$$

This linear relationship has an ordinate at the origin equal to unity in conformity with no synergy in the absence of AC_{Merk}. It illustrates the proportionality between the interfacial contact areas and the synergy factor R. For 2,4-D, the

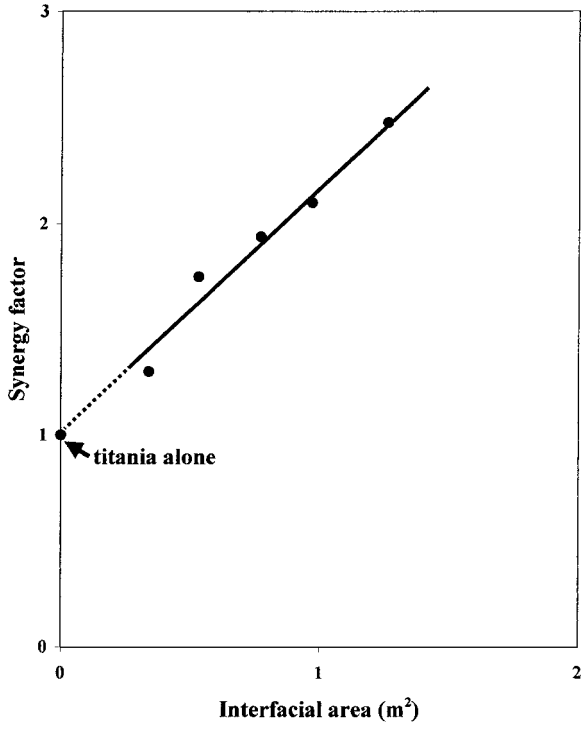

FIG. 7. Changes in factor R observed in phenol photodegradation as a function of the interfacial areas created between AC_M and different masses of TiO_2.

R factor is only equal to 1.3. However, because of solubility problems, the mass of AC_M used was twice smaller than that for phenol and 4-CP. A twice greater mass of AC_M would have provided a twice higher *R* factor (i.e., 2.6), close to the other two.

Electron microscopy of the TiO_2–AC mixture could have provided interesting information on the interphase. However, TEM requires sonication of the samples previous to their deposition on grids for a good examination, and it has been shown that sonication of a TiO_2-AC slurry was detrimental to photocatalysis (see Section 3.4.2 and Fig. 7) in Ref. 18. Therefore a TEM examination was not appropriate for a better characterization of the preferential contact TiO_2–AC. Nevertheless, TEM examinations of titania P-25 have already been carefully performed (35).

Another explanation for an apparent synergy effect can be based on the conventional Langmuir–Hinshelwood mechanism with the rate being proportional to the surface coverage θ varying as

$$r = k\theta = k\left\{K_{\text{ads}} \cdot C \Big/ \left(1 + K_{\text{ads}} \cdot C + \sum K_i C_i\right)\right\}.$$

Owing to the similarity of the reactants and of the main initial aromatic intermediates formed, the term $\sum K_i C_i$ can be estimated as constant, thus explaining the apparent first order:

$$r = k\theta = k\left\{K_{\text{ads}} \cdot C \Big/ \left(1 + K_{\text{ads}} C + \sum K_i C_i\right)\right\}$$
$$\cong k\left\{K_{\text{ads}} \cdot C \Big/ \left(1 + \sum K_i C_i\right)\right\} \cong k_{\text{app}} C.$$

The addition of a carbon powdered sorbent will reduce the sum $K_i C_i$ by partial adsorption of reactant and intermediates from solution, thus decreasing k_{app}. This positive effect outweighs the negative effect of some light absorption by the carbon. This absorption of light by AC is limited since (i) titania is five times more abundant in weight, thus playing the role of an inner filter, and (ii) the increase of temperature due to the absorption of light by AC in the slurry was found equal to only $\leq 1^\circ$C (see Section 3.2 in Ref. 18).

Another explanation could have been a better efficiency of titania originating from an improved UV absorbance of the slurry induced by a better dispersion—or a smaller agglomeration of the particles according to the pH induced by AC. We carefully performed a series of experiments and calculations inspired by Referee II, whose participation is acknowledged.

The results were the following:

(1)	TiO_2 slurry	pH = 5.27–5.33
(2)	AC Merck slurry	pH = 6.3
(3)	AC Purocarbon slurry	pH = 6.7
(4)	TiO_2 + AC Merck	pH = 5.06
(5)	TiO_2 + AC − PC	pH = 6.8–7

Then, we measured the UV absorbance of the slurries, using an incident UV-radiant flux equal to $\Phi_0 = 12$–34 mW/cm^2.

The absorbance of light by 50 mg titania slurry alone was 98.8% and increased to 99.7% when adding 10 mg AC. As announced in the text, the mass of 50 mg corresponded to a full absorbance of the radiant flux. The addition of AC did not seem to change the dispersion. It must be recalled that the "associative effect" between titania and AC_M was suppressed by sonication as mentioned in Section 4.2.1, which means that the destruction of titania–AC agglomeration or association is detrimental for photocatalysis.

Another question arises about the beneficial effect observed. The results in Fig. 1, obtained from experiments performed in triplicate with an excellent reproducibility indicated a non additivity of adsorption capacities of titania and AC, with a loss Δn of molecules adsorbed. In the case $TiO_2 + AC_M$, Δn_T was equal to 5.2×10^{-6} mol, i.e., 3×10^{18} sites lost by interaction. Taking into account (i) a mass of titania M = 50 mg, (ii) $\rho_{\text{titania}} = 3.85$ g/cm^3, (iii) S = 50 m^2/g, and (iv) the well-known formula for homodispersed nonporous particles:

$$d = 6/\rho S, \quad \text{with } d = \text{mean diameter} \quad (\text{or } R = 3/\rho S),$$

which was quite well observed on TEM micrographs showing a mean diameter of 30–32 nm (Fig. 1, Ref. 35), one could calculate the number *n* of titania spherical particles, contained in $M = 50$ mg and having an individual mass *m*, to be

$$n = M/m, \quad \text{with } m = 4/3\pi R^3 \rho, \quad \text{with } R = 3/\rho S,$$

thence,

$$n = (1/36\pi)\rho^2 S^3 = 8.2 \times 10^{14}.$$

The following question now arises: Can 8.2×10^{14} (or ca. 10^{15}) particles of titania block 3×10^{18} sites? For a tangential contact point between a spherical TiO_2 partilcle and AC, this assumption seems unreasonable. If 10^{15} particles block 3×10^{18} sites, this means that each particle blocks 3000 sites. If one admits a maximum density of 5×10^{18} sites/m^2 (or 5 sites/nm^2) on titania according to Boehm (36), 3000 sites represent 600 nm^2. Since one particle has a $\emptyset = 31$ nm, its surface *S* is equal to

$$S = 4\pi R^2 = \pi \mathrm{d}^2 = \pi \times (31)^2 = 3019 \approx 3000 \text{ nm}^2.$$

This means that 20% of the surface of titania is involved in the inhibition of phenol adsorption on the $TiO_2 + AC$ system. This ratio of 20% could appear more reasonable than the above number of 3000 phenol adsorption sites blocked per one titania particle. However, this titania–AC interaction could still appear untenable for blocking adsorption of phenol molecules 3–6 Å in diameter. Therefore additional

studies are necessary (i) to better elucidate the nonadditivity of phenol adsorption on titania + AC, which has been accurately and systematically observed on all samples, and (ii) to explain the positive association of titania and AC_{Merck}.

4.2.2. Inhibition Effects for TiO_2–AC_{PC}. Since factor R is smaller than unity for TiO_2–AC_{PC} in the three reactions studied, it has to be considered as an inhibition factor concerning phenol, 4-CP, and 2,4-D disappearance, although the estimated values of ΔS for TiO_2–AC_{PC} were higher than those for TiO_2–AC_M, for all the molecules studied. Moreover, the inhibition factors observed in the kinetics of phenol disappearance on UV-irradiated TiO_2–AC_{PC} were practically constant, independent of titania's masses added to this activated carbon, and therefore of ΔS. From Table 1, the main characteristics of AC_M and AC_{PC} appear to be different and have to be taken into account to explain the opposite photocatalytic behaviors between TiO_2–AC_M and TiO_2–AC_{PC}. Any interpreatation of the adsorptive behavior of activated carbons based solely on the magnitude of their surface area is incomplete because it is necessary to consider the relative pore size distribution (22–24).

A synergistic effect has been proposed by some of us for activated carbon-supported HDS catalysts (19, 25, 26) as consequence of a driving force (or "sink") functioning from the inside of slit micropores. In the present study, if we take into account the main pore width of each AC given in Table 1, the synergy effects observed on TiO_2–AC_M can be associated to an enhanced adsorption of the phenolic molecules from the solution into the AC_M slit micropores. Although the surface area of AC_M is significantly smaller than that of AC_{PC} (775 vs 1240 m^2/g), the total number of adsorption sites n_T belonging to AC_M and TiO_2–AC_M were higher than those obtained on AC_{PC} or TiO_2–AC_{PC}.

The surface chemistry of the present ACs must be considered with respect to adsorption of phenolic substances, since it is known that the mechanisms of adsorption are controlled by the nature of the surface functional groups of AC (27–30). The two presently activated carbons have been previously characterized (18, 19, 25, 31–34). From those studies, it was concluded that AC_M is an H-type activated carbon, while the AC_{PC} is an L-type activated carbon. The H-type active carbons are hydrophobic as a consequence of a surface with a basic nature that yields solutions with basic pH. On the contrary, L-type carbons are characterized by hydrophilic properties on account of the presence of surface acids and therefore yield acidic pH in solution.

Electrokinetic studies (24) have indicated that H-type activated carbons display a positive surface potential, which is opposite to the negative surface potential characteristic of L-type carbons. This negative surface potential is in line with the presence of acidic oxygen structures on the surface of AC.

Therefore, it can be assumed that phenol adsorption on AC_M occurs through its acidic proton, whereas on AC_{PC} the adsorption occurs through the π electrons of the aromatic ring. These mechanisms are in line with previous studies that reported an irreversible adsorption mechanism (28) involving oxidative coupling of phenolic substances by the acidic functional groups presented on L-type activated carbons (30). It must be noted that, as well as the irreversible mechanism of phenol adsorption, the possible evolution of noncommon intermediate products as a consequence of surface oxidative coupling reactions could be responsible of the inhibition effects observed on UV-irradiated TiO_2–AC_{PC}.

In parallel to what has been developed for TiO_2–AC_M, the "shadowing" effect due to light absorption by AC_{PC} outweighs any adsorption influence and causes a decrease in the overall rate.

4.3. Consequence of the Synergy Effect upon the Intermediate Products

The nature of the main intermediate products (hydroquinone and benzoquinone) is the same for TiO_2–AC as for neat TiO_2. This confirms that the reaction mechanism has not been altered nor changed by the addition of AC, which is photoinactive as shown in Fig. 2. UV photons create electron-hole pairs in titania,

$$TiO_2 + h\nu \rightarrow e^- + p^+, \quad [5]$$

which separate because of electron transfer reactions:

$$O_2 + e^- \longrightarrow O_{2^\circ^-}(\text{ads}) \quad [6]$$

$$OH + p^+ \longrightarrow OH^\circ. \quad [7]$$

The OH° radicals created react with phenolic compounds to produce hydroxylated aromatic compounds, mainly hydroquinone (Fig. 4; in equilibrium with benzoquinone), and then aliphatic fragments resulting from the ring opening before producing CO_2.

The synergy effect can also be pointed out in the kinetics of intermediate product appearance and disappearance. For hydroquinone, which is the main intermediate, its kinetics can be summarized as

$$R\text{–}C_6H_4\text{–}OH \xrightarrow{k_1} HQ \xrightarrow{k_2} BQ \xrightarrow{k_3} \cdots \xrightarrow{k_n} CO_2, \quad [8]$$

with R = H, Cl, or O–CH_2–COOH.

The formal reaction rate of formation of HQ is given by

$$r = d[HQ]/dt = k_1[R\text{–}C_6H_4\text{–}OH] - k_2[HQ]. \quad [9]$$

The integration of Eq. [9] gives

$$[HQ] = C_0[k_1/(k_2 - k_1)][\exp(-k_1 t) - \exp(-k_2 t)], \quad [10]$$

where C_0 is the initial concentration of the pollutants. According to Eq. [10], [HQ] goes through a maximum, whose coordinates are

$$t_{max} = [\ln(k_2/k_1)]/(k_2 - k_1) \quad [11]$$

$$[HQ]_{max} = C_0(k_1/k_2)^{k_2/(k_2-k_1)} = C_0\gamma^{1/(1-\gamma)}, \quad [12]$$

with $\gamma = k_1/k_2$, t_{max}, and $[HQ]_{max}$ being related by the equation

$$\ln(C_0/[HQ]_{max})/t_{max} = k_2. \quad [13]$$

The coordinates of the three maxima in [HQ] for neat TiO_2 and for TiO_2–AC taken in Fig. 4 enable one to calculate the corresponding values of k_1 and k_2. The addition of AC to titania increases the rate constant k_1 of HQ appearance by a factor equal to 1.82 for AC_M and to 1.3 for AC_{PC}. The rate constant k_2 of HQ disappearance is increased by a factor of 1.65 for AC_M but decreased by a factor of 0.75 for AC_{PC}. This clearly confirms that the synergy effect is acting on both k_1 and k_2 constants in the case of the TiO_2–AC_M mixture because of the strong adsorption of the intermediates on AC_M and because of their subsequent transfer to titania induced by an elevated concentration gradient acting as the driving force. This effect is still operating to a smaller extent for TiO_2–AC_{PC} for the disappearance of phenol and the appearance of hydroquinone, but the ratio $k_2(TiO_2$–$AC_{PC})/k_2(TiO_2)$ lower than unity (0.75) induces an overall inhibition effect. This is in line with the chemical nature of the intermediates and of the surface of AC_{PC} discussed above in Section 4.3.

5. CONCLUSIONS

The addition of a commercial H-type activated carbon to titania under UV irradiation induces a beneficial effect on the photocatalytic degradation of phenol, of 4-CP, and of herbicide 2,4-D by a factor of 2.5 in the photoefficiency of titania quantified by the apparent first-order rate constant. It has been explained by an important adsorption of the pollutants on AC followed by a mass transfer to photoactive titania through a common interface between AC and TiO_2. This interface is spontaneously created by a mere mixture of both phases in suspension.

In contrast, the addition of an L-type carbon is rather detrimental, which suggests that the AC properties play a significative role upon the photoefficiency of associated titania. Significant differences in intermediate product distributions were observed and ascribed to the characteristics of each AC, as a consequence of different mechanisms of adsorption of the phenolic substances.

The beneficial effect observed for TiO_2–AC_{MERCK} does not result from an artifact since the same R factor was found (i) for different pollutants and (ii) in the large-scale solar pilot plant at PSA.

From a practical point of view, it is possible to obtain clean water in a much shorter time than with titania alone. AC concentrates both the initial pollutant and its degradation intermediate products in close vicinity to titania thus enabling their transfer and decomposition on it. Such a system would be particularly efficient for the dexofication of large volumes of polluted waters, especially when using solar energy in the case of helio-photocatalysis in sunny arid areas all around the world.

ACKNOWLEDGMENTS

The authors thank the Franco-Venezuelian P.C.P program and Venezuelian CONICIT for their financial support.

REFERENCES

1. Schiavello, M. (Ed.), "Photocatalysis and Environment: Trends and applications," NATO ASI Series C, Vol. 238. Kluwer Academic, London, 1987.
2. Ollis, D. F., and Al-Ekabi, H. (Eds.), "Photocatalytic Purification and Treatment of Water and Air," Elsevier, Amsterdam, 1993.
3. Legrini, O., Oliveros, E., and Braun, A., *Chem. Rev.* **93**, 671 (1993).
4. Bahnemann, D., Cunningham, J., Fox, M. A., Pelizzetti, E., Pichat, P., and Serpone, N., *in* "Aquatic and Surface Photochemistry" (G. R. Zepp and D. G., Crosby, Eds.), Lewis, Boca Raton, FL, 1994.
5. Blake, D. M., Bibliography of work on the photocatalytic removal of hazardous compounds from water and air, NREL/TP-430-22197, National Renewable Energy Laboratory, Golden Co, 1997 and 1999.
6. Herrmann, J.-M., *Catal. Today* **53**, 115 (1999).
7. Herrmann, J. M., *in* "Environmental Catalysis" (F. Jansen and R. A. van Santen, Eds.), Catalytic Science Series, Vol. 1, Chap. 9, pp. 171–194. Imperial College Press, London, 1999.
8. Mu, W., Herrmann, J.-M., and Pichat, P., *Catal. Lett.* **3**, 73 (1989).
9. Herrmann, J.-M., Didier, J., and Pichat, P., *Chem. Phys. Lett.* **108**, 618 (1984).
10. Tanguay, J. F., Suib, S. L., and Coughlin, R. W., *J. Catal.* **117**, 335 (1989).
11. Minero, C., Catozzo, F., and Pelizzetti, E., *Langmuir* **8**, 489 (1992).
12. Takeda, N., Torimoto, T., Sampath, S., Kuwabata, S., and Yoneyama, H., *J. Phys. Chem.* **99**, 9986 (1995).
13. Ibuzuki, T., Kutsuma, S., and Takeuchi, K., in "Photocatalytic Purification and Treatment of Water and Air," (D. F. Ollis and H. Al-Ekabi, Eds.), Elsevier, Amsterdam, 1993.
14. Ibuzuki, T., and Takeuchi, K., *J. Mol. Catal.* **88**, 93 (1994).
15. Uchida, H., Itoh, S., and Yoneyama, H., *Chem. Lett.* 1995 (1993).
16. Torimoto, T., Itoh, S., Kuwabata, S., and Yoneyama, H., *Environ. Sci. Technol.* **30**, 1275 (1996).
17. Torimoto, T., Okawa, Y., Takeda, N., and Yoneyama, H., *J. Photochem. Photobiol. A: Chem.* **103**, 153 (1997).
18. Matos, J., Laine, J., and Herrmann, J.-M., *Appl. Catal. B: Environ.* **18**, 281 (1998).
19. Laine, J., Severino, F., Labady, M., and Gallardo, J., *J. Catal.* **138**, 145 (1992).
20. Matos, J., Brito, J. L., and Laine, J., *Appl. Catal. A: Gen.* **152**, 27 (1997).
21. Turchi, C. S., and Ollis, D. F., *J. Catal.* **119**, 483 (1989).
22. Mahajan, O. P., Moreno-Castilla, C., and Walker, P. L., Jr., *Sep. Sci. Technol.* **15**, 1733 (1980).
23. Castellan, G., *J. Amer. Chem. Soc.* **53**, 850 (1931).
24. Snoeyink, V. L., and Weber, W. J., Jr., *Environ. Sci. Technol.* **1**, 228 (1967).

25. Laine, J., Severino, F., and Labady, M., *J. Catal.* **147**, 355 (1994).
26. Laine, J., Labady, M., Severino, F., and Yunes, S., *J. Catal.* **166**, 384 (1997).
27. Magne, P., and Walker, Jr., P. L., *Carbon* **24**, 101 (1986).
28. Grant, T. M., and Judson King, C., *Ind. Eng. Chem. Res.* **29**, 264 (1990).
29. Vidic, R. D., and Suldan, M. T., *Environ. Sci. Technol.* **25**, 1612 (1993).
30. Vidic, R. D., Suldan, M. T., and Brenner, R. C., *Environ. Sci. Technol.* **27**, 2079 (1993).
31. Laine, J., and Yunes, S., *Carbon* **30**, 601 (1992).
32. Matos, J., Thesis, Lic., Universidad Central de Venezuela, Caracas, Venezuela, 1994.
33. Laine, J., Calafat, A., and Labady, M., *Carbon* **27**, 191 (1989).
34. Laine, J., and Calafat, A., *Carbon* **29**, 949 (1991).
35. Herrmann, J. M., *J. Catal.* **118**, 43 (1989).
36. Boehm, H. P., *Adv. Catal.* **16**, 179 (1966).